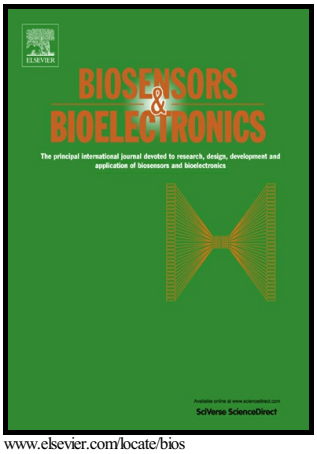

www.elsevier.com/locate/bios

A versatile label-free electrochemical biosensor for circulating tumor DNA based on dual enzyme assisted multiple amplification strategy

Hua-Feng Wang, Rong-Na Ma, Fei Sun, Li-Ping Jia, Wei Zhang, Lei Shang, Qing-Wang Xue, Wen-Li Jia, Huai-Sheng Wang

PII: S0956-5663(18)30719-X
DOI: https://doi.org/10.1016/j.bios.2018.09.028
Reference: BIOS10768

To appear in: *Biosensors and Bioelectronic*

Received date: 17 July 2018
Revised date: 28 August 2018
Accepted date: 7 September 2018

Cite this article as: Hua-Feng Wang, Rong-Na Ma, Fei Sun, Li-Ping Jia, Wei Zhang, Lei Shang, Qing-Wang Xue, Wen-Li Jia and Huai-Sheng Wang, A versatile label-free electrochemical biosensor for circulating tumor DNA based on dual enzyme assisted multiple amplification strategy, *Biosensors and Bioelectronic,* https://doi.org/10.1016/j.bios.2018.09.028

A versatile label-free electrochemical biosensor for circulating tumor DNA based on dual enzyme assisted multiple amplification strategy

Hua-Feng Wang[a 1], Rong-Na Ma[a1]*, Fei Sun[b], Li-Ping Jia[a], Wei Zhang[a], Lei Shang[a], Qing-Wang Xue[a], Wen-Li Jia[a], Huai-Sheng Wang[a,]*

[a]*School of Chemistry and Chemical Engineering, Liaocheng University, Liaocheng 252059, Shandong, P.R. China*

[b]*Oncology Department, Hospital of Traditional Chinese Medicine of Liaocheng City, Liaocheng 252000, Shandong, P.R. China*

marongna@lcu.edu.cn (R. N. Ma)
hswang@lcu.edu.cn (H. S. Wang)

[*]Corresponding author. Tel./Fax: +86-635-8239121.

Abstract:

A versatile label-free electrochemical biosensor based on dual enzyme assisted multiple amplification strategy was developed for ultrasensitive detection of circulating tumor DNA (ctDNA). The biosensor consists of a triple-helix molecular switch (THMS) as molecular recognition and signal transduction probe, ribonuclease HII (RNase HII) and terminal deoxynucleotidyl transferase (TdT) as dual enzyme assisted multiple amplification accelerator. The presence of target ctDNA could open THMS and trigger RNase HII-assisted homogenous target recycling amplification to produce substantial signal transduction probe (STP). The released STP hybridized with the capture probe immobilized on a gold electrode, then TdT and assistant probe were further employed to fulfill TdT-mediated cascade extension and generate stable DNA dendritic nanostructures. The electroactive methyl blue (MB) was finally used as the signal reporter to realize the multiple electrochemical amplification ctDNA detection as the amount of MB is positively correlated with the target ctDNA. Combined with the efficient recognition capacity of the designed THMS and the excellent multiple amplification ability of RNase HII and TdT, the constructed sensing platform could detect KRAS G12DM with a wide detection range from 0.01 fM to 1 pM, and the limit of detection as low as 2.4 aM. Besides, the platform is capable of detecting ctDNA in biological fluid such as plasma. More importantly, by substituting the loop of THMS with different sequences, this strategy could be conveniently

[1] Author Contributions. H.F.Wang and R.N.Ma contributed equally to this work.

expanded into the detection of other ctDNA, showing promising potential applications in clinical cancer screening and prognosis.

Keywords: Electrochemical biosensor; Circulating tumor DNA; Dual enzyme assisted multiple amplification

1. Introduction

Cancer is one of the leading causes of death worldwide, by 2030, it is projected that the number of cancer sufferers will increase to 24.6 million and the number of cancer deaths will up to 13 million (Atun and Cavalli, 2018). Therefore, the early identification and real-time screen neoplastic changes are of great significance to avoid premature deaths, unnecessary suffering and achieve the most effective management and the highest survival chance (Cohen et al., 2017). Liquid biopsy, a simple and non-invasive alternative to surgical biopsies, have attracted intensive interest as it could prevent notorious pain, lethal complication or infection and expensive expenses of tissue biopsies and facilitate efficient diagnosis, prognostic analysis, and patient follow-up (Alix-Panabières and Pantel, 2016; Brock et al., 2017; Crowley et al., 2017; Heitzer et al., 2015). Several promising biomarkers including protein markers (e.g. prostate specific antigen, carcinoembryonic antigen and alpha fetoprotein, thrombin) (Ju, 2017; Zong et al., 2015; Gao et al., 2016), intact circulating tumor cells (Cao et al., 2017 Shen et al., 2016; Sun et al., 2016; Zhai et al., 2017), circulating tumor DNA (ctDNA) (Rodda et al., 2018; Zhang et al., 2018; Zhou et al., 2016; Zou et al., 2017) and circulating cell fragments such as exosomes (Haber and Velculescu, 2014; Su, 2015) have been discovered in the blood and widely applied to diagnose or monitor diseases.

Circulating tumor DNA (ctDNA), is single-stranded or double-stranded tumor-derived fragmented DNA in the peripheral blood which may associate with tumor burden, intratumoral

heterogeneity and therapeutic effect, has gained traction for its potential clinical early diagnosis and real-time monitoring (Ignatiadis et al., 2015; Jahr et al., 2001; Lebofsky et al., 2015; Stroun et al., 2001). Therefore, liquid biopsy based on ctDNA has shed a new light to accurately determine the tumor progression, prognosis and assist in targeted therapy, because it would provide a more effective, real-time and patient-friendly method for the diagnose, monitoring and treatment of cancer (Chi et al., 2016; Jamal-Hanjani et al., 2017; Wan et al., 2017). To date, several methods involving DNA sequencing (Gale et al., 2016; Ståhlberg et al.,2016), polymerase chain reaction (Freidin et al., 2015; Zhu et al., 2017), surface-enhanced Raman spectroscopy (Wee et al., 2016; Zhou et al., 2016), and localized surface plasmon resonance (Nguyen and Sim, 2015) have been reported for analysis of ctDNA. Among them, electrochemical strategies have attracted considerable attention due to their prominent features of simple operation, rapid response, low cost, and compatibility with micromanufacturing technology (Das et al., 2015; Das et al., 2016). Kelley et al. firstly reported an electrochemical clamp assay that could successfully detect circulating nucleic acids in serum (Das et al., 2015). However, the research is just in the starting stage and provide a lot of space for follow-up development, and it is still a persistent challenge to develop a versatile and facile ctDNA electrochemical detection strategy with easy operation and low consumption in early cancer screening and evaluation.

Herein, a versatile label-free electrochemical sensing strategy was firstly developed for highly sensitive detection of KRAS G12DM single-stranded ctDNA based on terminal deoxynucleotidyl transferase (TdT) and ribonuclease HII (RNase HII) dual enzyme assisted multiple amplification to form a dendritic structure (Scheme 1). The specially designed triple-helix molecular switch (THMS) was employed as the recognition and signal transduction

element to realize the RNase HII-assisted homogenous target recycling amplification and release numerous signal transduction probe (STP). The released STP could be conveniently introduced to the electrode surface and trigger the first-step TdT-mediated extension to form the DNA "trunk". Then, the specially designed assistant probe (AP), which could partially hybridize with the DNA "trunk" and partially initiate the second-step TdT-mediated extension, was introduced to generate a long stable DNA dendritic structure to decorate redox-active MB and achieve efficient sensitivity. The proposed strategy possesses some remarkable features: First, the introduction of RNase HII leading to the highly efficient 1:N target-responsive recycling and numerous STP releases. Second, by separating the molecular recognition element and signal reporter, the strategy is generalizable and different ctDNAs detection requirement just need to alter the loop of label-free recognition probe (RP) in THMS. Third, the unique design by integrating RNase HII-assisted homogenous target recycling amplification and TdT-mediated cascade extension to amplify signals could realize the ultrahigh sensitivity. Therefore, the proposed strategy provides a universal and versatile tool for ctDNA and holds a great potential for highly sensitive target analysis and clinical noninvasive liquid biopsy.

2. Experimental

2.1. Materials and reagents

All oligonucleotides were synthesized, HPLC-purified and freeze-dried by Sangon Biotech. Co., Ltd. (Shanghai, China). Their sequences are given in Table S1 (Supporting Information). Tris (2-carboxyethyl) phosphine hydrochloride (TCEP), tris (hydroxymethyl) aminomethane (Tris) and 6-Mercapto-1-hexanol (MCH) were obtained from Sigma-Aldrich (USA). Terminal deoxynucleotidyl transferase (TdT) and ribonuclease HII (RNase HII) were purchased from New England Biolabs, Inc. (Beijing, China). Deoxythymine triphosphate (dTTP) and

3-morpholinopropanesulfonic acid (MOPS) were obtained from Sangon Biotech. Co., Ltd. (Shanghai, China). Methylene blue (MB) were purchased from Shanghai Reagent Co. (Shanghai, China). All these reagents were used as received without further purification. Human plasma samples were provided by Liaocheng People's Hospital and Hospital of Traditional Chinese Medicine of Liaocheng City. Ultrapure water obtained from a Millipore water purification system (≥18 MΩ, Milli-Q, Millipore) was used in all assays.

2.2. Apparatus

The high-resolution transmission electron microscopic (HRTEM) image was observed on a Talos F200X (FEI, USA) with an accelerating voltage of 200 kV. Atomic force microscopy (AFM) was performed on a Bruker Multimode 8 atomic force microscope. The electrochemical measurements were conducted on a CHI 760C electrochemical workstation (CH Instruments Inc., U.S.A.) with a conventional three-electrode system composed of a platinum wire as counter, Ag/AgCl as reference and the Au electrode as working electrode, respectively. Electrochemical impedance spectroscopic measurements were carried out on a Zahner Zennium pro (Zahner, Germany).

2.3. Fabrication of the sensing platform

Gold electrode (~2 mm diameter, CH Instrument Inc.) was polished carefully to a mirror surface with aqueous slurry of 0.3 μm diameter alumina particles and then successively washed in an ultrasonic cleaner with water and ethanol. The electrode was then cleaned by immersing into the fresh piranha solution (H_2SO_4:H_2O_2=3:1, v/v) for 10 min, flushed with water, and dried under a nitrogen stream. Finally, the gold electrodes were electrochemically polished in 0.5 M H_2SO_4 by scanning the potential from -0.2 to +1.6 V at scan rate of 0.1 V/s for 40 cycles. Then, the obtained gold electrode was washed with ultrapure water thoroughly and dried under

flowing nitrogen.

CP (10 μM) was firstly incubated with equal volume of freshly prepared TCEP (1 mM) for 1 h to cleave the disulfide bonds. The reduced CP was subsequently diluted with 25 mM Tris-HCl buffer (pH 7.4, 100 mM NaCl and 5 mM $MgCl_2$, the same below) to obtain a final concentration of 0.5 μM reduced CP. Then 6 μL of the above solution was dropped on the pretreated electrode to incubate at RT for 2 h, rinsed thoroughly with 25 mM Tris-HCl buffer to remove unbounded CP and dried with nitrogen. The electrode was then incubated with 6 μL of 1 mM MCH for 1 h to block the unmodified sites. After another washing and drying operation, the CP-modified electrochemical sensing platform was obtained and stored at 4 °C in the Tris-HCl buffer before use.

2.4. Procedure for ctDNA assay

Before target ctDNA (T1) recognition, the THMS was formed by adding 3 μL of 5 μM RP to 3.3 μL of 5 μM STP in 10 mM MOPS buffer (pH 5.0, 150 mM NaCl) and incubating at 23 ^{o}C for 1 h. The RNase HII-assisted homogeneous target recycling amplification was fulfilled by incubating the obtained THMS, 6 U RNase HII and T1 with different concentrations (T1 was firstly dissolved in ultrapure water to obtain the 100 μM storage solution. Then, a series of different concentration dilutions was obtained by ten-fold serial dilution.) in 1×NEBuffer 1 at 37°C for 1 h. Then 6 μL of the obtained solution was incubated with the CP-modified electrode at 37 °C for 1 h to allow the released signal transduction probes (STP) hybridize with CP, followed by washing and drying operation, 6 μL of reaction mixture (Solution I) containing 10 mM dTTP, 2 U of TdT, 1×TdT Reaction Buffer (pH 7.9, 50 mM potassium acetate, 20 mM Tris-acetate, 10 mM magnesium acetate), 0.25 mM $CoCl_2$ (The addition of Co^{2+} in the reaction makes tailing more efficient.) was dropped onto the electrode and incubated at 37 ^{o}C for 1 h to

realize the first-step TdT-mediated extension and obtain the DNA "trunk". After washing with Tris-HCl buffer and drying with nitrogen, 6 μL of 10 μM AP was dropped and incubated for 1 h at 37 ^{o}C, after another washing and drying, 6 μL of Solution I was dropped again and incubated for 1 h at 37 ^{o}C to fulfill the second-step TdT-mediated extension and obtain the DNA dendritic structure. Furthermore, it was incubated in 1 mM MB at 37 ^{o}C for 30 min to ensure the combination between MB and the dendritic DNA. After every step above mentioned, these modified electrodes were extensively rinsed with ultrapure water and dried under a stream of nitrogen prior to electrochemical characterization. The whole procedure was shown in Scheme 1. The differential pulse voltammogram (DPV) was recorded with a step potential of 4 mV, a frequency of 25 Hz, and an amplitude of 25 mV by scanning the potential window from 0.2 V to -0.6 V in 25 mM Tris-HCl buffer. Electrochemical impedance spectroscopic measurements were carried out in 5 mM $[Fe(CN)_6]^{4-/3-}$ (1:1) solution containing 0.1 M KCl. The formal potential of the redox probe $[Fe(CN)_6]^{4-/3-}$ is 220 mV. Unless specifically noted, the experiments were carried out at the room temperature.

2.5. Extraction of ctDNA from plasma

The freshly collected blood samples supplied by healthy donor (HD) and colorectal cancer patient (CRCP) were immediately extracted in anticoagulant tubes and centrifuged to obtain plasma. DNA was isolated using QIAamp DNA Blood Mini Kit (Qiagen, Germany) following the manufacturer's handbook. The procedure was described tersely as follows: First, 200 μL plasma was mixed and incubated with 20 μL protease and 200 μL Lysis buffer at 56 ^{o}C for 10 min to obtain a homogeneous lysate, centrifuged and added 200 μL ethanol, then centrifuged again to remove drops. Second, spin column was used for extraction, centrifuged at 8000 rpm for 1 min, then 200 μL two types of washing buffers were successively used to improve the

purity of the extracted DNA. Finally, 200 μL Elution buffer was added and incubated at room temperature for 5 min, and centrifuged at 8000 rpm for 1 min to obtain the enriched DNA and stored at -20 °C.

3. Results and discussion

3.1. Principle of the proposed biosensor

The principle of the proposed dual enzyme assisted multiple amplification biosensor is schematically illustrated in Scheme 1. The whole design consisted of three key elements: (1) The triple-helix molecular switch (THMS), which served as both molecular recognition element and signal transduction unit, was tactfully constructed by signal transduction probe (STP) and recognition probe via Watson-Crick (-) and Hoogsteen (•) base pairings in a particular situation (Salunkhe et al., 1992; Zheng et al., 2011; Iacovelli et al., 2017). With the aid of RNase HII, the homogeneous target ctDNA recognition disassembles the THMS and releases numerous STP, which could fulfill target recycling amplification and signal transduction. (2) The released STP could be captured by the capture probe attached electrode and trigger the first-step TdT-mediated DNA polymerase to form a long single stranded DNA resembling "trunk" as TdT can catalyzes the addition of dNTP at the 3'-OH terminus of DNA molecules (Hu et al., 2015). (3) The specially designed assistant probe (AP) was further introduced to initiate the second-step TdT mediated extension and form branch-like DNA to decorate redox-active MB. Thus, the total amount of target is proportional to the amount of redox mediators of MB and the accordingly electrochemical signal. This approach can achieve multiple amplification since one copy of the target can yield a MB-decorated DNA tree via strong electrostatic interaction. Most important, this strategy is convenient and generalizable as the platform can be readily extended to detect a wide range of ctDNA only by changing the

loop sequence of RP, and thus possesses great potential for universal gene-related molecular diagnostics.

3.2. Characterization of the biosensor

Polyacrylamide gel electrophoresis (PAGE), HRTEM, AFM and electrochemical impedance spectroscopy (EIS) were firstly performed to characterize the biosensor construction. As proof-of-principle, the TdT-mediated cascade extension was firstly examined. As shown in Figure 1A, CP and STP exhibited individual clear band, respectively (lanes 1 and 2). A new band which moved obviously slower than both STP and CP was appeared, indicating that STP and CP could hybridize to form a cooperative complex (lane 3). After the CP/STP complex was firstly incubated with TdT and dTTP, an obvious change in the band shift was appeared (lane 4), indicating the first-step TdT-mediated extension occurred. Furthermore, the second-step TdT-mediated extension is further confirmed by the large increase molecular weight of product (lane 5). These results effectively confirmed that the designed TdT-mediated extension can be successfully realized.

Direct imaging of the assembled products by HRTEM and AFM further confirmed the PAGE results. The HRTEM image in Figure 1B shows that large-scale dendric nanostructures with different size were formed. The observed dendritic structure of the assembled products is evidently visual evidence that the TdT-mediate DNA extension indeed occurred as designed. A positive AFM image also present the expected dendritic morphology of the assembled products (Figure 1C), which further confirmed the successful TdT-mediate DNA amplification. Notably, the sizes and the morphologies were polydispersity as a result of the random multi-dimension assembly of substrates. By extensively analysis of the HRTEM and AFM, it could undoubtedly confirm the proposed TdT-mediate DNA amplification took place as anticipated.

Electrochemical impedance spectroscopy (EIS) was employed to characterize the electrochemical fabrication and amplification process as it has been proven to be one of the most powerful tools to investigate the interfacial reaction mechanism of electrode surface (Figure 1D). The impedance data were fitted to an equivalent electronic circuit, shown as the inset in Figure 1D, which includes the electrolyte solution resistance R_s, the surface electron transfer resistance R_{ct} that reflects the surface property of the electrode surface, the Warburg impedance Z_w, resulting from diffusion of the redox probe; and the constant phase element related to double layer capacitance C_{dl} (Gao, 2015). Compared with bare Au electrode (curve a), the CP modified Au electrode exhibited increased electron-transfer resistance R_{ct} (curve b) because the repelling force of the introduced negatively charged phosphate backbone of DNA toward $[Fe(CN)_6]^{3-/4-}$, which reflected the successful immobilization of CP. Subsequently, surface blocking with MCH led to a further increase in R_{ct} due to the insulativity of MCH (curve c). Subsequent STP hybridization and first extension by TdT led to further increase in R_{ct} (curve d and e), suggesting the successful TdT-assisted first-step amplification. After the AP was captured and second extension by TdT, the R_{ct} were further enhanced (curve f and g), which can be attributed to the repulsive force between DNA dendric structure and the negatively charged redox couple. All these experimental results indicate that the modification and subsequent TdT-mediate DNA extension has been successfully accomplished according to Scheme 1.

3.3. Feasibility of the biosensing method

To demonstrate the feasibility of the designed dual enzyme assisted multiple amplification strategy for ctDNA detection, DPV obtained upon analyzing the target ctDNA (T1) in the presence of dual enzyme (RNase HII+TdT) and those obtained in a series of control

experiments are depicted in Figure 2. Either THMS (curve b) or the mixture of THMS+RNase HII (curve c) incubate with the sensing platform shows almost similar weak I_{MB} as the MCH/CP/Au electrode (curve a), which indicates that THMS are hardly open and release STP to trigger the following TdT meidiated extension without T1. However, as hypothesized, the presence of T1+THMS+RNase HII (curve d), or TdT extension/T1+THMS(curve e) could induce the different levels of I_{MB} increase, as a result of the different controlling condition would trigger a proportionately electrochemical signal amplification. A further increase of I_{MB} was observed when the presence of TdT extension/T1+THMS+RNase HII (curve f), implying that the dendritic structure has been successfully obtained and the multiple amplification is more efficient for the signal enhancement. These results clearly confirm that the sequential amplification of RNase HII followed by TdT extension is the preferred strategy for the detection of ctDNA.

3.4. Optimization of experimental conditions

The optimization of CP concentration and homogenous reaction time was conducted to achieve excellent analytical performance. The packing density of CP immobilized on the gold electrode could drastically affect the analytical performance of proposed biosensor and was controlled by varying the concentration of thiolated CP during sensor fabrication. Higher density would induce electrostatic repulsion and steric hindrance, which increased the painful interaction between neighbouring CP and hindered the hybridization between CP and STP. While the lower packing density may decrease the detection efficiency. As shown in Figure 3A, the I_{MB} increased correspondingly with increasing the CP concentration up to 0.5 μM, and then gradually declined with further increase of the CP concentration. Therefore, 6 μL of 0.5 μM CP was selected for the next experiments. The MB incubation time was another considerable

parameter affected the performance of the proposed biosensor. It could be seen that the I_{MB} increased continuously with the incubation time and almost reached the saturation value at a short incubation time of about 30 min (Figure 3B), indicating that 30 min was sufficient for MB incubation to fulfill the decorate of DNA dendric structure.

3.5. Analytical performance

Under the optimal conditions, the analytical performance of the proposed biosensor was investigated by varying the target T1 concentration. As shown in Figure 4A, the I_{MB} increase obviously with the increase of target T1 concentrations, demonstrating that the increasing concentration of released STP and TdT-mediated generated dendritic structure bring a great amount of MB adsorbed on the electrode and produce a remarkable amplified electrochemical signal. Figure 4B shows that the I_{MB} exhibited a good linear relationship with the logarithm value of target T1 concentration within the concentration range of 5 orders of magnitude from 0.01 fM to 1 pM. The correlation equation was I (μA) = 3.853 + 0.6374lg [C_{Target}/pM] (R=0.9995) with a limit of detection down to 2.4 aM (S/N = 3). The analytical characteristics of the present biosensor was also compared with some previous detection strategies, and the results were given in Table S2 (Supporting Information). Apparently, the proposed dual enzyme assisted multiple amplification mechanism has higher efficiency with lower detection limitation and relatively wide detection range.

In order to substantiate the excellent analytical performance of the dual enzyme assisted multiple amplification strategy, control experiments in the absence of RNase HII were carried out. As shown in Figure 4C and D, the intensity of the I_{MB} increased in proportion to the T1 concentration from 1 fM to 0.01 nM with the detection limit of 0.05 fM. Obviously, the dual enzyme assisted multiple amplification extends the linear range for 1 order of magnitude and

decreases the LOD for 1 order, which gaves an immediate evidence for the feasibility of our amplification strategy by combined the RNase HII amplification with the extension reaction of TdT. The DPV responses of the same concentration were also compared between dual enzyme and single enzyme assisted amplification (Figure S1, Supporting Information). And the result shows that the proposed dual enzyme assisted amplification exhibited higher I_{MB} than that of the single enzyme assisted amplification at the same concentration, which further confirmed the superiority of the proposed strategy.

3.6. Specificity, reproducibility and stability of the biosensor

The specificity of the proposed strategy was based on the accuracy of RNase HII, which can only recognize and act on the perfectly matched DNA/RNA hybridization. In light of the unique characters of RNase HII, the specificity of this assay toward mutated target T1 was examined by mixing T1 and wild-type T2 together in different molar ratios (T2:T1 = control, 1000:1, 500:1, 200:1, 50:1, 10:1, which control group only had T2) with a total concentration of 10 fM. The detailed results are illustrated in Figure S2 (Supporting Information). As expected, the proposed strategy shows the satisfactory capability of capturing and recognizing low abundance of mutations from abundant wild-type sequences. The excellent selectivity of the proposed sensing strategy was due to the high specificity of RNase HII to special perfectly matched RNA/DNA as well as the ingenious design to perform the recognition-amplification event.

To investigate the reproducibility of the biosensing system, three different concentrations of T1 were repeatedly measured by identical batches of modified electrodes (Table S3, Supporting Information). The relative standard deviations (RSD) for three paralleled detection of 0.01 fM, 0.01 pM and 0.1 pM were 5.49%, 5.98% and 7.43%, respectively, indicating

acceptable precision and satisfactory reproducibility of the biosensor. Additionally, the proposed biosensor exhibited satisfactory stability. After long-term storage (4 °C in the Tris-HCl buffer) bioactive assay, as much as 93% (two weeks) of the initial response was preserved, demonstrating the proposed biosensor could be used for ctDNA analysis with acceptable stability.

3.7. Real sample analysis of ctDNA

Encouraged by the unprecedented sensitivity and wide linear detection range of the proposed biosensor, plasma samples collected from 5 CRCPs and 5 HDs were employed to evaluate the capability in the real world. The point mutations of single stranded KRAS G12DM were usually chosen as the diagnostic biomarker because the activating mutations of the KRAS gene usually occurred in CRCPs. Figure 5 shows the result of direct detection single stranded KRAS G12DM in plasma, the electrochemical peak currents of all 5 CRCPs is significantly higher than that for the HDs, indicating that KRAS G12DM has a high expression level in the colorectal cancer patient blood and the constructed platform provides outstanding sensitivity and specificity. The concentrations of single-stranded KRAS G12DM in plasma were further calculated according to the calibration curve in the inset of Figure 4B. As shown in Table S4 (Supporting Information), the median concentration of KRAS G12DM from 5 CRCP plasma samples (0.19 fM) is distinctly higher than that of the HDs (11.59 aM). These results demonstrated that the expression levels of KRAS G12DM can provide a new diagnostic biomarker for liquid biopsy and thus the proposed strategy possesses a huge potential for applications in the clinical diagnosis.

4. Conclusions

In summary, a versatile label-free electrochemical biosensor based on RNase HII and TdT dual enzyme assisted multiple amplification strategy was developed for ultrasensitive detection ctDNA. A powerful integration of THMS and double enzyme assisted multiple amplification made it possible to directly detect ctDNA such as KRAS G12DM as low as aM level with a linear range of 5 orders of magnitude, which could rival or even exceed that of the reported excellent electrochemical biosensors. Moreover, it exhibited satisfactory specificity and acceptable accuracy and can be readily extended to detect a wide range of ctDNA with just change the loop sequence of the recognition probe. Thus, this work opens a promising avenue to develop the label-free biosensing system and has great potential for versatile application in noninvasive liquid biopsy.

Acknowledgements

This work was financially supported by the National Natural Science Foundation of China (21505063, 21375055, 21405070, 21427808) and Natural Science Foundation of Shandong Province (ZR2015BQ007, ZR2017BB084, ZR2017QB010).

Appendix A. Supporting information

Supplementary data associated with this article can be found in Supporting Information.

References

Alix-Panabières, C., Pantel, K., 2016. Cancer Discov. 6, 479–91.

Atun, R., Cavalli, F., 2018. Lancet 391, 412–413.

Brock, G., Castellanos-Rizaldos, E., Hu, L., Coticchia, C., Skog, J., 2015. Transl. Cancer Res. 280–290.

Cao, J., Zhao, X. -P., Younis, M. R., Li, Z. -Q., Xia, X. -H., Wang, C., 2017. Anal. Chem. 89, 10957–10964.

Chi, K. R., 2016. Nature 532, 269−271.

Cohen, J. D., Javed, A. A., Thoburn, C., Wong, F., Tie, J., Gibbs, P., Schmidt, C. M., Yip-Schneider, M. T., Allen, P. J., Schattner, M., Brand, R. E., Singhi, A. D., Petersen, G. M., Hong, S.-M., Kim, S. C., Falconi, M., Doglioni, C., Weiss, M. J., Ahuja, N., He, J., Makary, M. A., Maitra, A., Hanash, S. M., Molin, M. D., Wang, Y., Li, L., Ptak, J., Dobbyn, L., Schaefer, J., Silliman, N., Popoli, M., Goggins, M. G., Hruban, R. H., Wolfgang, C. L., Klein, A. P., Tomasetti, C., Papadopoulos, N., Kinzler, K. W., Vogelstein, B., Lennon, A. M., 2017. Proc. Natl. Acad. Sci. USA 114, 10202–10207.

Crowley, E., Nicolantonio, F. D., Loupakis, F., Bardelli, A., 2013. Nat. Rev. Clin. Oncol. 10, 472–480.

Das, J., Ivanov, I., Montermini, L., Rak, J., Sargent, E. H., Kelley, S. O., 2015. Nat. Chem. 7, 569−575.

Das, J., Ivanov, I., Sargent, E. H., Kelley, S. O., 2016. J. Am. Chem. Soc. 138, 11009−11016.

Freidin, M.B., Freydina, D.V., Leung, M., Fernandez, A.M., Nicholson, A.G., Lim, E., 2015. Clin. Chem. 61, 1299−1304.

Gale, D., Plagnol, V., Lawson, A., Pugh, M., Smalley, S., Howarth, K., Madi, M., Durham, B.,

Kumanduri, V., Lo, K., Clark, J., Green, E., Rosenfeld, N., Forshew, T., 2016. Cancer Res. 76, 3639.

Gao, F., Du, L., Zhang, Y., Zhou, F., Tang, D., 2016. Biosens. Bioelectron. 86, 185–193.

Gao, F., Qian, Y., Zhang, L., Dai, S., Lan, Y., Zhang, Y., Du, L., Tang, D., 2015. Biosens. Bioelectron. 71, 158–163.

Haber, D. A., Velculescu, V. E., 2014. Cancer Discov. 4, 650–661.

Heitzer, E., Ulz, P., Geigl, J. B., 2015. Clin. Chem. 61, 112–123.

Hu, Y. F., Shen, Q. P., Wang, L., Liu, Z. L., Nie, Z., Yao, S. Z., 2015. Biosens. Bioelectron. 63, 331–338.

Iacovelli, F., Idili, A., Benincasa, A., Mariottini, D., Ottaviani, A., Falconi, M., Ricci, F., Desideri, A., 2017. J. Am. Chem. Soc. 139, 5321−5329.

Ignatiadis, M., Lee, M., Jeffrey, S. S., 2015. Clin. Cancer Res. 21, 4786−4800.

Jahr, S., Hentze, H., Englisch, S., Hardt, D., Fackelmayer, F. O., Hesch, R. D., Knippers, R., 2001. Cancer Res. 61, 1659−1665.

Jamal-Hanjani, M., Wilson, G. A., McGranahan, N., Birkbak, N. J., Watkins, T. B. K., Veeriah, S., 2017. N. Engl. J. Med. 376, 2109−2121.

Ju, H., 2017, J. Anal. Test. 1, 7.

Lebofsky, R., Decraene, C., Bernard, V., Kamal, M., Blin, A., Leroy, Q., Frio, T. R., Pierron, G., Callens, C., Bieche, I., Saliou, A., Madic, J., Rouleau, E., Bidard, F.-C., Lantz, O., Stern, M.-H., Tourneau, C. L., Pierga, J.-Y., 2015. Mol. Oncol. 783−790.

Nguyen, A. H., Sim, S. J., 2015. Biosens. Bioelectron. 67, 443−449.

Rodda, A. E., Parker, B. J., Spencer, A., Corrie, S. R., 2018. ACS Sens. 3, 540−560.

Salunkhe, M., Wu, T. F., Letsinger, R. L., 1992. J. Am. Chem. Soc. 114, 8768−8772.

Shen, H. W., Yang, J., Chen, Z. P., Chen, X. P., Wang, L., Hu, J., Ji, F. H., Xie, G. M., Feng, W. L., 2016. Biosens. Bioelectron. 81, 495−502.

Ståhlberg, A., Krzyzanowski, P. M., Jackson, J. B., Egyud, M., Stein, L., Godfrey, T. E., 2016. Nucleic Acids Res. 44, e105.

Stroun, M., Lyautey, J., Lederrey, C., Olson-Sand, A., Anker, P., 2001. Clin. Chim. Acta. 313, 139−142.

Su, J., 2015. ACS Photonics 2, 1241−1245.

Sun, N., Li, X. P., Wang, Z. L., Zhang, R. H., Wang, J. N., Wang, K. W., Pei, R. J., 2016. ACS Appl. Mater. Interfaces 8, 12638−12643.

Wan, J. C. M., Massie, C., Garcia-Corbacho, J., Mouliere, F., Brenton, J. D., Caldas, C., Pacey, S., Baird, R., Rosenfeld, N., 2017. Nat. Rev. Cancer 17, 223−239.

Wee, E. J. H., Wang, Y., Tsao, S. C., Trau, M., 2016. Theranostics 6, 1506−1513.

Zhai, T. T., Ye, D., Zhang, Q. W., Wu, Z. Q., Xia, X. H., 2017. ACS Appl. Mater. Interfaces 9, 34706−34714.

Zhang, W., Dai, Z., Liu, X., Yang, J., 2018. Biosens. Bioelectron. 105, 116−120.

Zheng, J., Li, J. S., Jiang, Y., Jin, J. Y., Wang, K. M., Yang, R. H., Tan, W. H., 2011. Anal. Chem. 83, 6586−6592.

Zhou, Q., Zheng, J., Qing, Z., Zheng, M., Yang, J., Yang, S., Ying, L., Yang, R., 2016. Anal. Chem. 88, 4759−4765.

Zhu, Q., Xu, Y., Qiu, L., Ma, C., Yu, B., Song, Q., Jin, W., Jin, Q., Liu, J., Mu, Y., 2017. Lab Chip 17, 1655−1665.

Zong, C., Wu, J., Liu, M., Yan, F., Ju, H., 2015. Chem. Sci. 6, 2602−2607.

Zou, Z., Qi, P., Qing, Z., Zheng, J., Yang, S., Chen, W., Yang, R., 2017. Trends Anal. Chem. 97,

36–49.

Figure captions:

Scheme 1

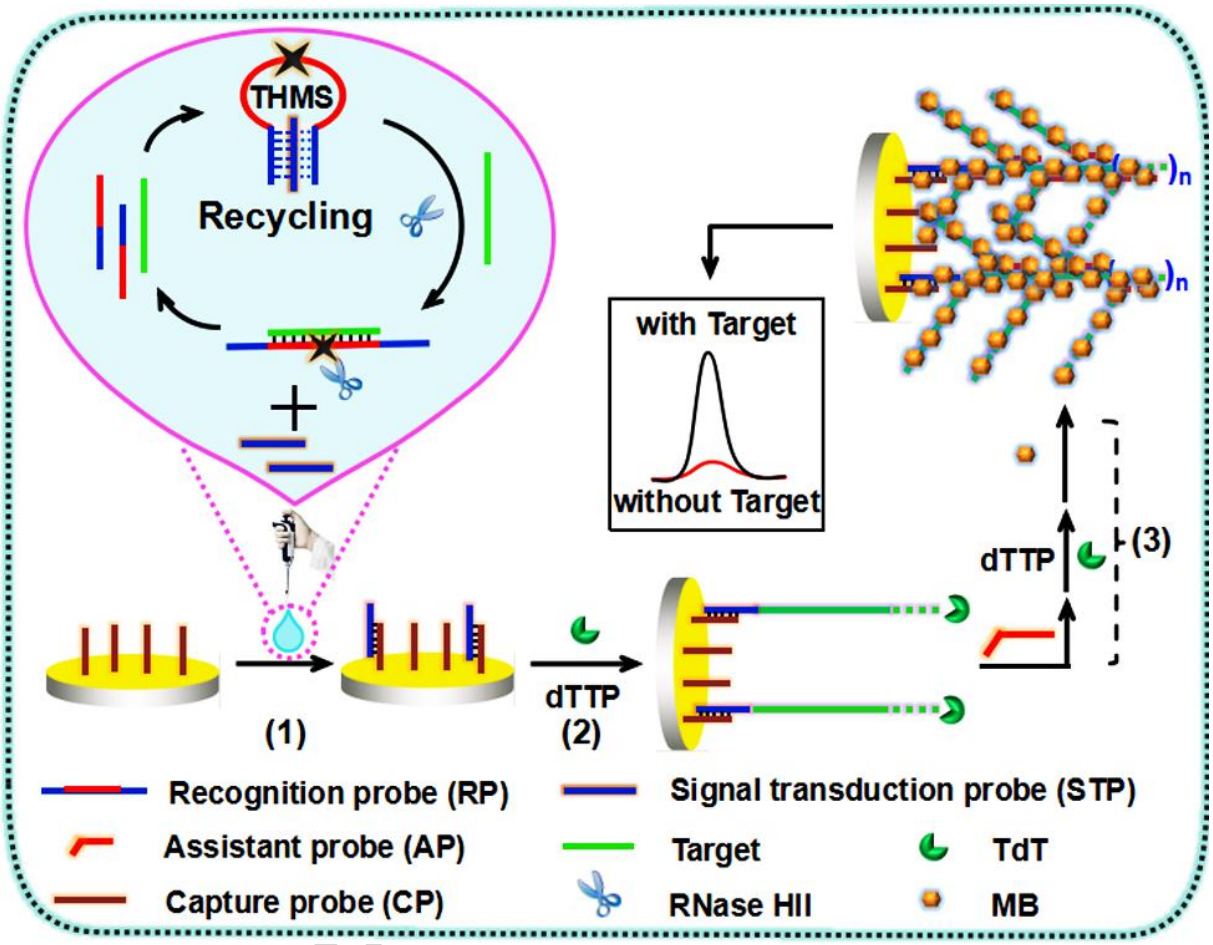

Fig. 1

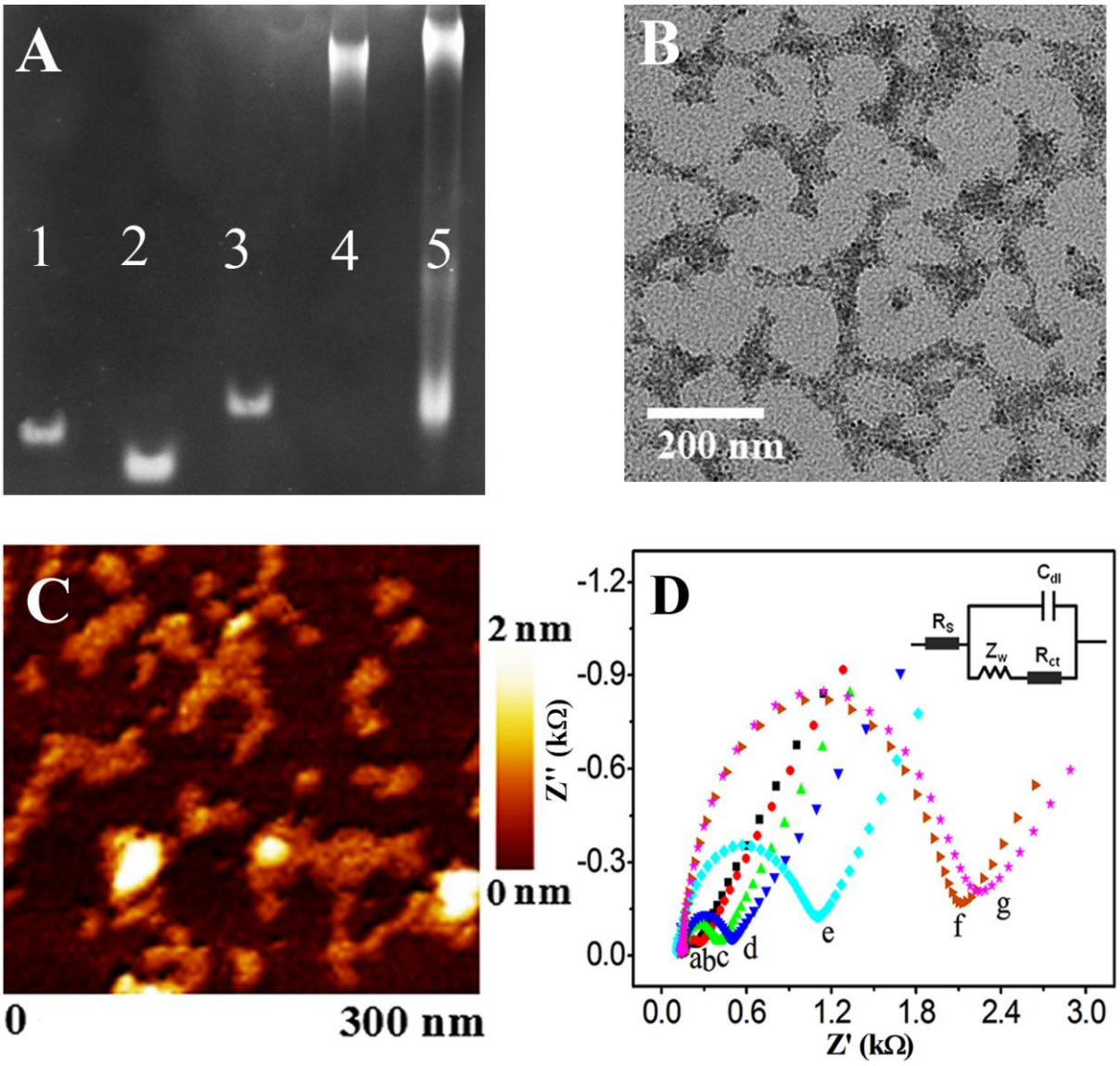
A
1
2
3
4
5
B
200 nm
C
2 nm
0 nm
0
300 nm
D
Z'' (kΩ)
Z' (kΩ)
-1.2
-0.9
-0.6
-0.3
0.0
0.0
0.6
1.2
1.8
2.4
3.0
abc
d
e
f
g
C_{dl}
R_S
Z_w
R_{ct}

Fig. 2

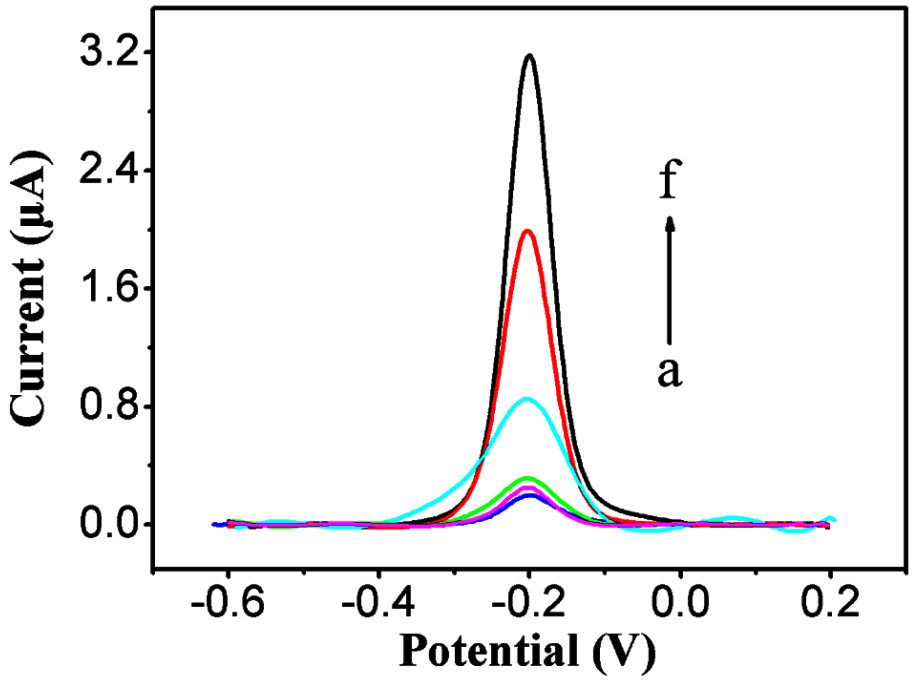
Current (μA)
Potential (V)
f
a
3.2
2.4
1.6
0.8
0.0
-0.6
-0.4
-0.2
0.0
0.2

Fig. 3

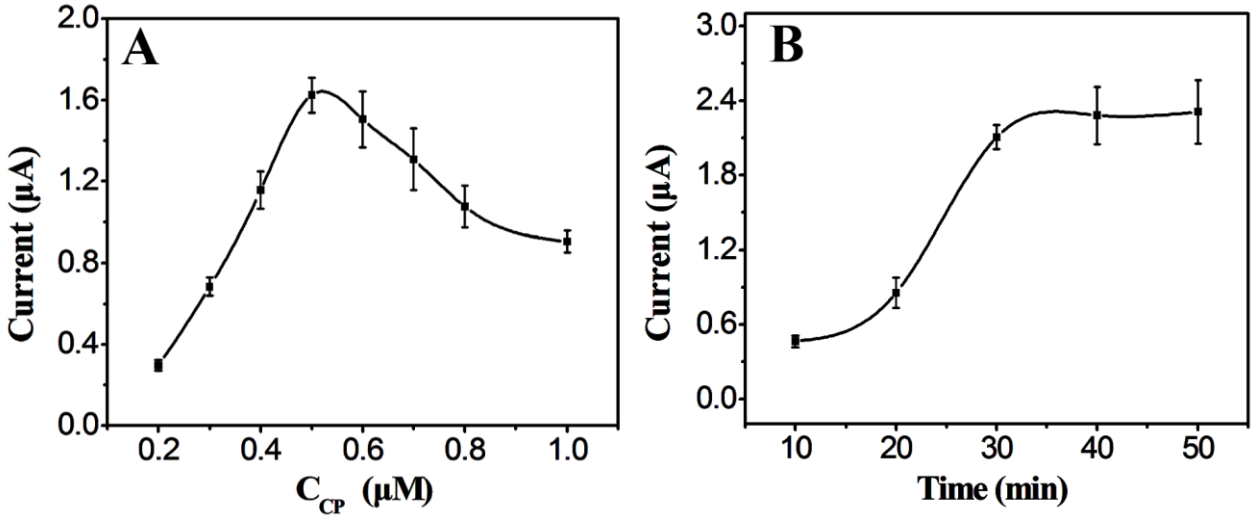
A
Current (μA)
C_{CP} (μM)
2.0
1.6
1.2
0.8
0.4
0.0
0.2
0.4
0.6
0.8
1.0
B
Current (μA)
Time (min)
3.0
2.4
1.8
1.2
0.6
0.0
10
20
30
40
50

Fig. 4

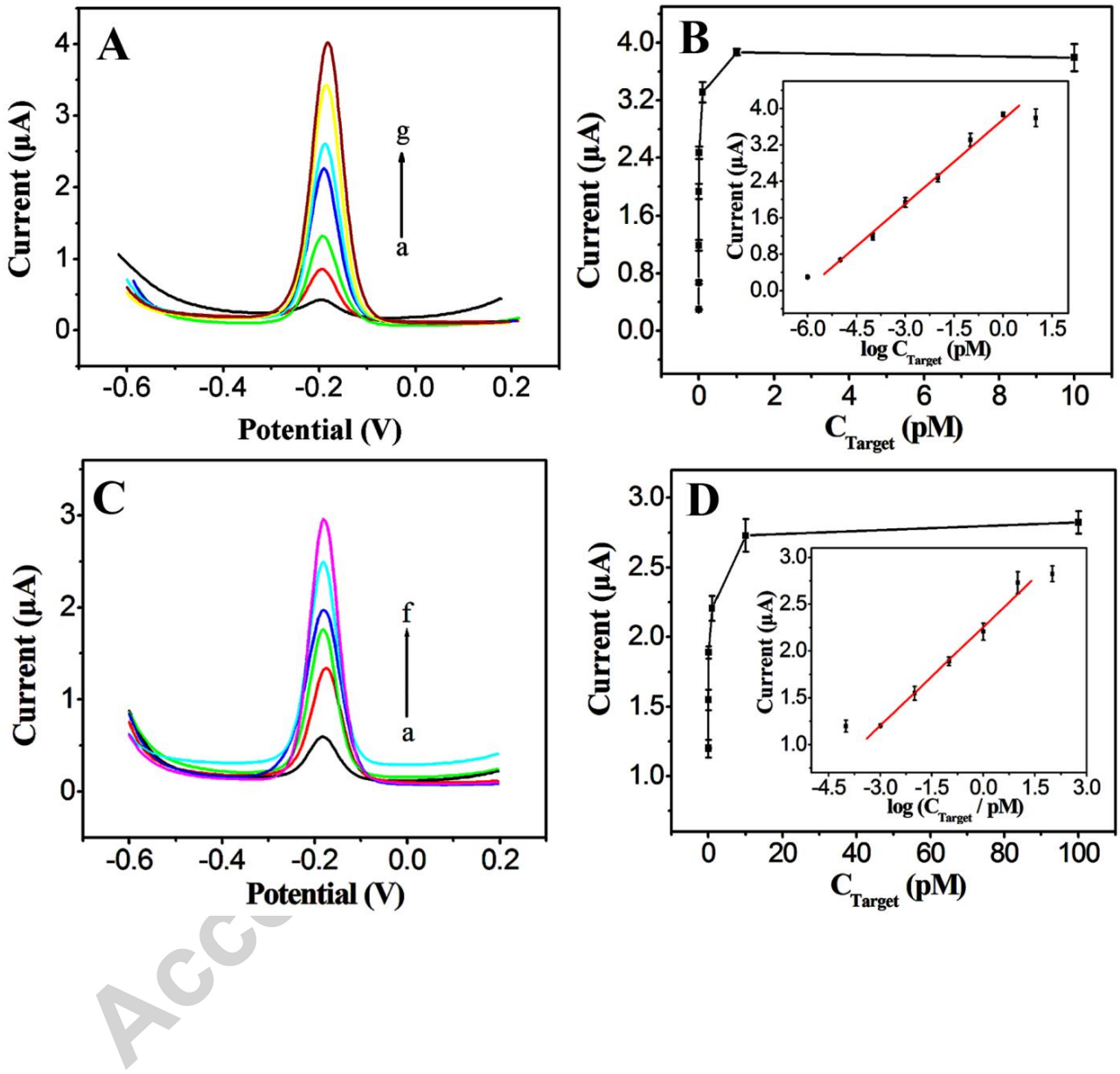
A
Current (μA)
Potential (V)
g
a
B
Current (μA)
C Target (pM)
log C Target (pM)
C
Current (μA)
Potential (V)
f
a
D
Current (μA)
C Target (pM)
log (C Target / pM)

Fig. 5

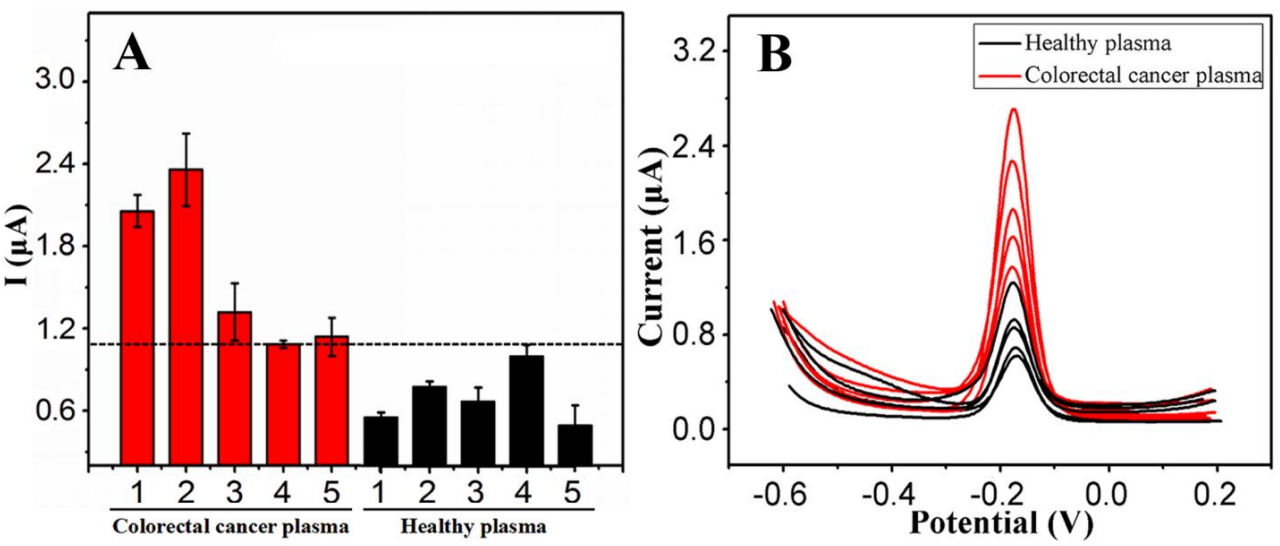

Highlights

- A versatile label-free electrochemical biosensor is developed by integrating RNase HII-assisted homogeneous target recycling amplification and TdT-mediated cascade extension.
- The biosensor can detect target ctDNA down to aM level with a dynamic range spanning 5 orders of magnitude.
- The biosensor can directly detect target ctDNA in biological fluid such as plasma.
- The detection platform can be readily extended to detect a wide range of ctDNA by substituting the loop of THMS with different sequences.

Figure captions:

Scheme 1 Schematic illustration of the dual enzyme assisted multiple amplification electrochemical biosensor.

Fig. 1. (A) PAGE analysis of TdT mediated extension. Lanes 1–5 represent STP, CP, CP/STP, the first-step TdT-mediated extension product and the second-step TdT-mediated extension product, respectively; (B) HRTEM image of the assembled dendritic DNA; (C) AFM image of the assembled dendritic DNA; (D) EIS of (a): Bare Au electrode, (b): CP/Au electrode, (c): MCH/CP/Au electrode, (d): (c) was incubated with T1+THMS+RNase HII, (e): the first-step TdT-mediated extension of (d), (f): (e) was incubated with AP and (g): the second-step TdT-mediated extension of (f).

Fig. 2. DPV responses of MB adsorbed at the biosensor surface under different conditions: (a) MCH/CP/Au electrode, (b) (a) was incubated with THMS, (c) (a) was incubated with THMS+RNase HII, (d) (a) was incubated with T1+THMS+RNase HII, (e) (a) was incubated with T1+THMS and extension by TdT and (f) (a) was incubated with T1+THMS+RNase HII and extension by TdT.

Fig. 3. Effects of (A) CP concentrations, and (B) the MB incubation time. The error bars represented the standard deviation of three measurements.

Fig. 4. (A) DPV responses for the detection of target ctDNA at concentrations of 0, 0.01 fM, 0.1 fM, 1 fM, 0.01 pM, 0.1 pM, and 1 pM (from a to g) with dual enzyme assisted multiple amplification, (B) Linear relationship between I_{MB} and logarithm of target ctDNA with dual enzyme assisted multiple amplification, (C) DPV curves for the detection of ctDNA at concentrations of 0, 1 fM, 0.01 pM, 0.1 pM, 1 pM, and 0.01 nM (from a to f) without RNase HII-assisted target recycling amplification, (D) Linear relationship between I_{MB} and logarithm

of target ctDNA without RNase HII-assisted target recycling amplification. Error bars represent standard deviations of three parallel experiments.

Fig. 5. (A) Histogram of detection of KRAS G12DM in clinical plasma using the proposed dual enzyme assisted multiple amplification electrochemical biosensor. Clinical samples were collected from 5 CRCP and 5 HD (control). The dashed line represents the minimum mean concentration of KRAS G12DM in CRCP plasma. (B) DPV responses for corresponding detection of KRAS G12DM of (A) in the same color. Error bars show the standard deviations of three independent measurements.